

Cite this: *RSC Adv.*, 2017, 7, 31338

Received 28th April 2017

Accepted 12th June 2017

DOI: 10.1039/c7ra04807f

rsc.li/rsc-advances

# Binding behaviour of a 12-mer peptide and its tandem dimer to gymnospermae and angiospermae lignins†

Satoshi Oshiro, ‡<sup>a</sup> Asako Yamaguchi ‡<sup>ab</sup> and Takashi Watanabe \*<sup>a</sup>

The binding behaviour of a 12-mer peptide and its tandem dimer to gymnospermae, *Cryptomeria japonica* and angiospermae, *Eucalyptus globulus* lignins was analysed. The tandem dimer significantly changed its conformation upon addition of the lignins to have a 10-times higher affinity than the 12-mer peptide. This result exhibits potential for use as a molecular tool in lignin-degrading (bio)catalysts.

Lignin, accounting for 15–35% of the lignocellulose weight from plant biomass, is a three-dimensional polymer constructed from phenylpropanoid subunits interlinked by ether and carbon-carbon bonds.<sup>1,2</sup> Lignin contributes to the physical, biological and chemical stability of the plant cell wall by forming a matrix to cover the crystalline cellulose and hemicelluloses.<sup>3</sup> For the production of biofuels and chemicals from lignocellulosic materials by enzymatic saccharification and fermentation, pre-treatment of biomass is essential to increase the accessibility of hydrolases to the cell wall polysaccharides.<sup>4</sup> A number of physical, physicochemical, chemical and biological pre-treatment methods have been applied to disintegration of lignocellulosic biomass prior to the enzymatic saccharification.<sup>5–9</sup> From the view of biorefinery utilizing all biomass components, the production of aromatic chemicals from lignin is also important.<sup>10–13</sup> Therefore, a number of chemical and biological approaches have been studied, but lignin degradation is still challenging due to its highly recalcitrant chemical and physical structure.<sup>14</sup> Improvement of the affinity for lignin is a significant approach to facilitate the degradation activity of lignin-degrading (bio)catalysts with high selectivity. The lignin-binding module such as the carbohydrate-binding module (CBM) in cellulolytic enzymes was not discovered in natural proteins.<sup>15,16</sup> We recently found some lignin-binding 12-mer peptide sequences using the phage display technique.<sup>17</sup> These peptides have the potential for use as novel tools that improve the lignin affinity to lignin-degrading catalysts and enzymes. The increase in affinity of the peptide to lignin is important for higher specific recognition of the lignin-degrading (bio)catalysts through the peptide moiety.

Lignin-degrading enzymes, lignin peroxidase, manganese peroxidase, versatile peroxidase and laccase extract one electron directly from polymeric lignin or through mediators. In the lignin-degradation through direct contact of the enzymes or the aid of diffusible mediators, enzymes should be located at a site close to the vicinity of the substrate because the life span of highly reactive radicals is very short, and the active radicals readily react with various organic molecules. This is true for synthetic catalysts degrading lignin by radical reactions.

In this study, we aimed to improve the affinity of the lignin-binding peptide through tandem dimerisation by bridging the two lignin-binding peptide sequences *via* a glycine residue or a 6-aminocaproic acid residue because the multimerisation of a peptide is effective for obtaining higher affinity and activity.<sup>18,19</sup> Furthermore, for the detailed analysis of the peptide binding mechanism to lignins from gymnospermae and angiospermae, we observed differential conformational changes of the peptides upon recognition of milled-wood lignins (MWLs) from *C. japonica* (CMWL) and *E. globulus* (EMWL) using attenuated total reflection-Fourier transform infrared (ATR-FTIR) spectroscopy. The effect of tandem dimerisation and interaction of the monomer and dimeric 12-mer peptides with the lignins is discussed.

## Affinity analysis of the tandem 12-mer peptide dimers to lignins

First, we designed the two tandem dimer peptides (Table 1). C416dimer\_1 was composed of two C416 sequences and a glycine residue that was located between two C416 sequences as a linker residue. C416dimer\_2 had 6-aminocaproic acid as a longer linker residue instead of the glycine residue.

The dissociation constants ( $K_D$ ) of C416dimer\_1 peptide to CMWL and EMWL were 10.1  $\mu$ M and 10.7  $\mu$ M, respectively (Table 1 and Fig. 1). The affinity of the dimer peptide was 10-times higher than that of monomeric C416 peptide. The  $K_D$  value of C416dimer\_2 was unchanged in comparison with that

<sup>a</sup>Research Institute for Sustainable Humanosphere, Kyoto University, Gokasho Uji, Kyoto 611-0011, Japan. E-mail: twatanab@rish.kyoto-u.ac.jp

<sup>b</sup>Department of Biological Science, Graduate School of Science, Osaka Prefecture University, 1-1 Gakuen-cho, Naka-ku, Sakai, Osaka 599-8531, Japan

† Electronic supplementary information (ESI) available: Materials and methods. See DOI: 10.1039/c7ra04807f

‡ These authors contributed equally.



Table 1 Sequences of C416 monomer peptide and C416 dimer peptides

Peptide	Sequence	Dissociation constant ( $K_D$ ) [M]	
		CMWL	EMWL
C416	HFPSPIFQRHSH	$1.47 \times 10^{-4}$	$1.32 \times 10^{-4}$
C416dimer_1	HFPSPIFQRHSHGHFPSPIFQRHSH	$1.01 \times 10^{-5}$	$1.07 \times 10^{-5}$
C416dimer_2	HFPSPIFQRHSH-6AA <sup>a</sup> -HFPSPIFQRHSH	$1.00 \times 10^{-5}$	$8.68 \times 10^{-6}$

<sup>a</sup> 6AA: 6-aminocaproic acid.

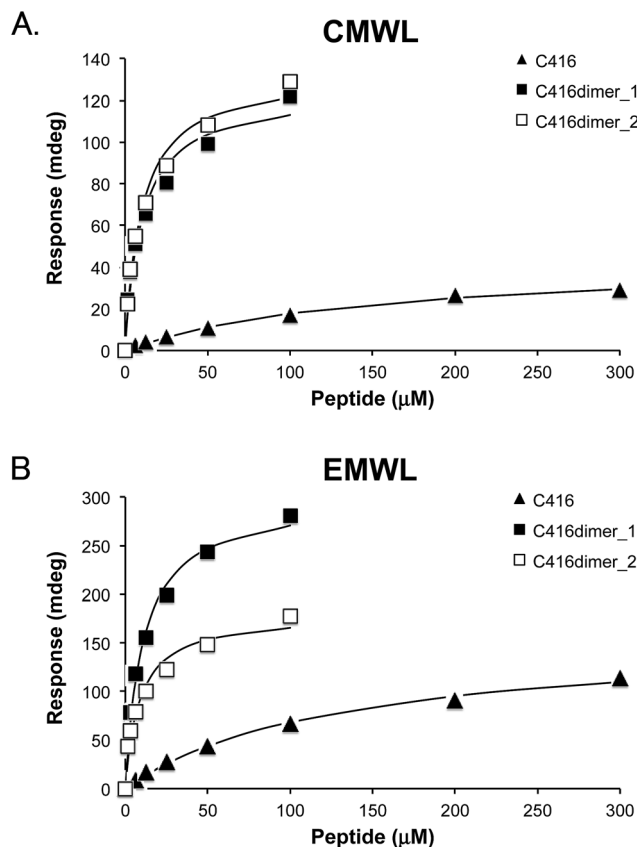


Fig. 1 Surface plasmon resonance (SPR) equilibrium analysis of C416 (closed triangles), C416dimer\_1 (closed squares) and C416dimer\_2 (open squares) binding to immobilized MWLs. The upper figure shows peptides binding to immobilized CMWL, and the lower figure shows peptides binding to immobilized EMWL.

of C416dimer\_1; thus, the length of the linker region hardly affected the affinity of the tandem dimer peptides.

## Secondary structure of the tandem dimer peptide and the monomer peptide

Second, we compared the secondary structures of C416dimer\_1 with that of the C416 monomer by measuring the circular dichroism (CD) and ATR-FTIR spectra. Both CD spectra of C416dimer\_1 and that of monomeric C416 indicated a negative peak at approximately 200 nm. The shape of the spectra

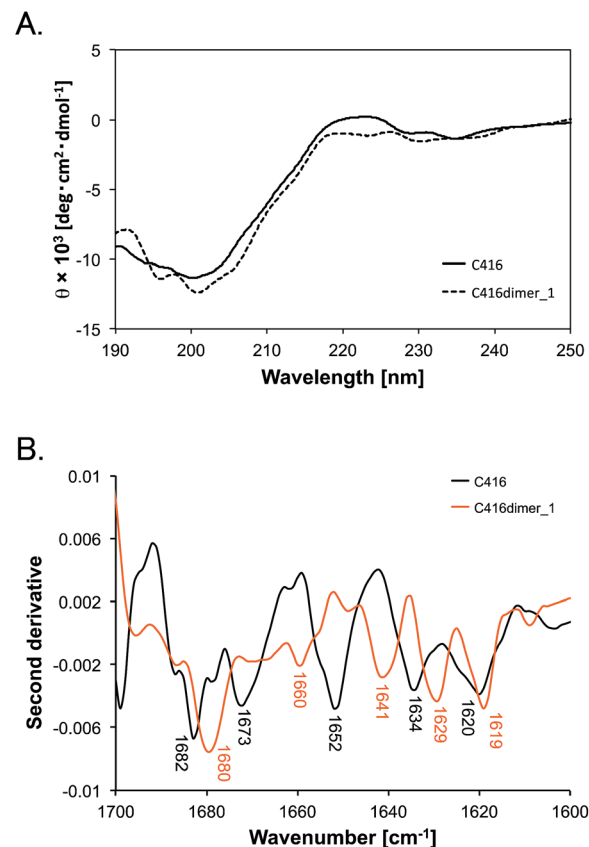


Fig. 2 (A) CD spectra of C416 (solid line) and C416dimer\_1 (dashed line). The samples (75 μM C416 and 30 μM C416dimer\_1) were dissolved in 10 mM sodium phosphate (pH 7.0). The spectra were measured at 20 °C. (B) Second derivative of the ATR-FTIR spectra of C416 (black line) and C416dimer\_1 (orange line). 10 mM C416 peptide or 5 mM C416dimer\_1 peptide was dissolved in PBS (pH 7.0) and the spectra were measured at room temperature.

reflected that the main structures of C416dimer\_1 and monomeric C416 were random coil (Fig. 2A). We measured the ATR-FTIR spectra in the amide I region (1600–1700 cm<sup>-1</sup>) of peptides and assigned the secondary structure from the second derivative peaks of the spectra (Fig. 2B and Table 2).

Monomeric C416 peptide showed peaks at 1620, 1634, 1652, 1673 and 1682 cm<sup>-1</sup>. Although the IR peaks in the 1620–1640 cm<sup>-1</sup> region could reflect both a β-sheet or extended structure,<sup>20</sup> we assigned the peaks at 1620 and 1634 cm<sup>-1</sup> to the extended structure because the CD spectra provided no evidence for a β-sheet structure in the peptide. The peak at 1652 cm<sup>-1</sup> was



Table 2 Assignment of secondary structure of peptides from the peaks of second derivative of ATR-FTIR spectra<sup>a</sup>

Peptide	Extended	Random	Turn
C416	1620, 1634	1652	1673, 1682
C416 + CMWL	1610, 1626, *1640	*1640, 1659	1675, 1678, 1690
C416 + EMWL	1618, 1629	1654	1673, 1678, 1683
C416dimer_1	1619, 1629	1641, *1660	*1660, 1680
C416dimer_1 + CMWL	1611, 1626, *1640	*1640	1661, 1675, 1679, 1691
C416dimer_1 + EMWL	1618, 1630, 1633	1654	1664, 1675

<sup>a</sup> \*The peak at 1640 cm<sup>-1</sup> could be assigned to an extended structure and a random structure. \*\*The peak at 1660 cm<sup>-1</sup> could be assigned to a random structure and a turn structure.

assigned to the random coil structure and the peaks at 1673 and 1682 cm<sup>-1</sup> were assigned to the turn structure.<sup>21</sup>

The spectrum of the C416dimer\_1 showed peaks at 1619, 1629, 1641, 1660 and 1680 cm<sup>-1</sup>. The area of the peak at 1680 cm<sup>-1</sup> accounted for the largest area in the spectra. The increase of the 1680 cm<sup>-1</sup> peak suggested that the turn structure is dominant in C416dimer\_1. Furthermore, the peak shift (1652 to 1641 cm<sup>-1</sup>) observed in C416dimer\_1 indicated a structural change in the random structure region.

Although marked structural differences were not found by CD spectra between C416dimer\_1 and C416 monomer, ATR-FTIR spectra indicated the changes in the conformation of the peptide through the tandem dimerisation. ATR-FTIR spectra in the amide I region reflects the stretching vibrations of C=O

bonds in the amide bonds, thus minor structural changes in random structure region could be detected.<sup>22</sup> The structural differences through the tandem dimerisation would affect the increased affinity to MWLs.

## Structural change of the lignin-binding peptides upon the addition of lignins

We observed the change of the ATR-FTIR spectra of peptides upon the addition of MWLs. In the CMWL-added condition, the shape of the spectra from the C416 peptide was dramatically changed. The peak at 1652 cm<sup>-1</sup> disappeared, and peaks at 1640, 1659 and 1690 cm<sup>-1</sup> appeared (Fig. 3A). These changes suggested that the random structure was altered to a turn

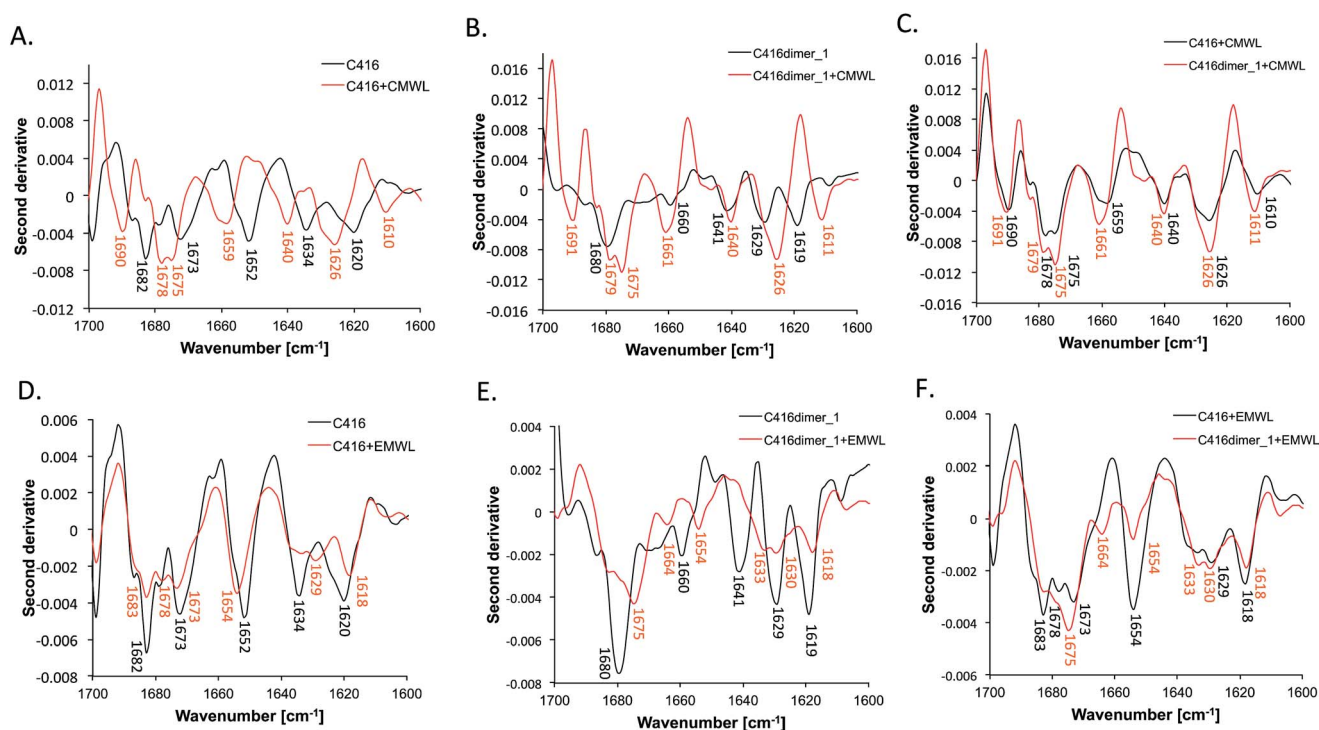


Fig. 3 Second derivative of ATR-FTIR spectra (1600–1700 cm<sup>-1</sup>) obtained from C416 and C416dimer\_1 peptides: (A) 10 mM C416 in the absence (black line) and presence (orange line) of 1 mg ml<sup>-1</sup> CMWL. (B) 5 mM C416dimer\_1 in the absence (black line) and presence (orange line) of 1 mg ml<sup>-1</sup> CMWL. (C) 10 mM C416 in the presence of 1 mg ml<sup>-1</sup> CMWL (black line) and 5 mM C416dimer\_1 in the presence of 1 mg ml<sup>-1</sup> CMWL (orange line). (D) 10 mM C416 in the absence (black line) and presence (orange line) of 1 mg ml<sup>-1</sup> EMWL. (E) 5 mM C416dimer\_1 in the absence (black line) and presence (orange line) of 1 mg ml<sup>-1</sup> EMWL. (F) 10 mM C416 in the presence of 1 mg ml<sup>-1</sup> EMWL (black line) and 5 mM C416dimer\_1 in the presence of 1 mg ml<sup>-1</sup> EMWL (orange line). All measurements were conducted at room temperature.



structure. The occurrence of the peak at  $1610\text{ cm}^{-1}$  indicated an extended structure with stronger intermolecular hydrogen bonds.<sup>23</sup> In addition, the shapes of the C416 and C416dimer\_1 spectra were very similar (Fig. 3B and C). The spectra showed that the C416dimer\_1 peptide took on a conformation that resembled the binding conformation of the C416 monomeric peptide upon CMWL recognition. In the EMWL-added C416 monomeric peptide, the spectral change was negligible as compared with the spectra of the peptide in the presence of CMWL. The major difference was the peak at  $1634\text{ cm}^{-1}$  was lost and a peak at  $1629\text{ cm}^{-1}$  appeared, suggesting a conformational change in the extended region (Fig. 3D). Surprisingly, the shape of the spectra obtained from EMWL-added C416dimer\_1 was significantly changed and different from the shape of the spectra from EMWL-added C416 monomer peptide (Fig. 3E and F). This suggested that the mechanism of peptide affinity enhancement by dimerisation was different in EMWL recognition from CMWL recognition. The different structural changes in peptides upon MWL recognition were caused by the structural differences between CMWL and EMWL.

Lignin from gymnospermae (softwood), including *C. japonica*, are mostly composed of guaiacyl units.<sup>1</sup> In contrast, lignin from *E. globulus*, classified as angiospermae (hardwood), is composed of syringyl units and guaiacyl units.<sup>1,24</sup> Previous studies have shown that the replacement of the Phe7 residue with isoleucine decreases the affinity of the C416 peptide for CMWL, but it does not affect the affinity for EMWL.<sup>17</sup> Therefore, the C416 12-mer peptide strongly recognized the structural differences in lignins from gymnospermae and angiospermae by changing the conformation of the peptide chain. Understanding of the flexible molecular recognition mechanism of C416 peptide and its tandem dimer would contribute to the synthesis of lignin-degrading (bio)catalysts with higher affinity and specificity to the lignin from various plant species.

## Conclusions

We enhanced the affinity of lignin-binding peptide C416 10-fold through tandem dimerisation. ATR-FTIR spectra revealed that the tandem dimerisation affected the peptide conformation. Furthermore, both monomeric and tandem dimer peptides took on different conformations upon CMWL binding and EMWL binding.

The tandem dimer peptide is expected to be a molecular tool for carrying lignin-degrading (bio)catalysts to lignin for the highly selective lignin degradation of lignocellulosic biomass.

## Acknowledgements

This research was supported by CREST (JPMJCR11B4), Japan Science and Technology Agency and collaborative project of RISH, Kyoto University.

## Notes and references

- 1 K. V. Sarkanen and C. H. Ludwig, *Lignins Occur. Form. Struct. React.*, 1971.
- 2 R. Pettersen, *Chem. solid wood*, 1984, pp. 1–9.
- 3 R. Vanholme, B. Demedts, K. Morreel, J. Ralph and W. Boerjan, *Plant Physiol.*, 2010, **153**, 895–905.
- 4 N. Pareek, T. Gillgren and L. J. Jönsson, *Bioresour. Technol.*, 2013, **148**, 70–77.
- 5 P. Bajpai, *Pretreatment of Lignocellulosic Biomass for Biofuel Production*, Springer Singapore, Singapore, 2016.
- 6 S. I. Mussatto, *Biomass Fractionation Technologies for a Lignocellulosic Feedstock Based Biorefinery*, Elsevier, Amsterdam, 2016.
- 7 A. K. Kumar and S. Sharma, *Bioresources and Bioprocessing*, 2017, **4**, 7.
- 8 J. N. Putro, F. E. Soetaredjo, S.-Y. Lin, Y.-H. Ju and S. Ismadji, *RSC Adv.*, 2016, **6**, 46834–46852.
- 9 Z. Zhang, M. D. Harrison, D. W. Rackemann, W. O. S. Doherty and I. M. O'Hara, *Green Chem.*, 2016, **18**, 360–381.
- 10 V. Menon and M. Rao, *Prog. Energy Combust. Sci.*, 2012, **38**, 522–550.
- 11 C. Li, X. Zhao, A. Wang, G. W. Huber and T. Zhang, *Chem. Rev.*, 2015, **115**, 11559–11624.
- 12 P. C. A. Bruijninx and B. M. Weckhuysen, *Nat. Chem.*, 2014, **6**, 1035–1036.
- 13 A. Kaiho, M. Kogo, R. Sakai, K. Saito and T. Watanabe, *Green Chem.*, 2015, **17**, 2780–2783.
- 14 X. Zhao, L. Zhang and D. Liu, *Biofuels, Bioprod. Biorefin.*, 2012, **6**, 465–482.
- 15 A. B. Boraston, D. N. Bolam, H. J. Gilbert and G. J. Davies, *Biochem. J.*, 2004, **382**, 769–781.
- 16 D. Guillén, S. Sánchez and R. Rodríguez-Sanoja, *Appl. Microbiol. Biotechnol.*, 2010, **85**, 1241–1249.
- 17 A. Yamaguchi, K. Isozaki, M. Nakamura, H. Takaya and T. Watanabe, *Sci. Rep.*, 2016, **6**, 21833.
- 18 A. N. Singh, M. J. McGuire, S. Li, G. Hao, A. Kumar, X. Sun and K. C. Brown, *Theranostics*, 2014, **4**, 745–760.
- 19 D. L. Johnson, F. X. Farrell, F. P. Barbone, F. J. McMahon, J. Tullai, D. Kroon, J. Freedy, R. A. Zivin, L. S. Mulcahy and L. K. Jolliffe, *Chem. Biol.*, 1997, **4**, 939–950.
- 20 T. F. Kumosinski and J. J. Unruh, *Talanta*, 1996, **43**, 199–219.
- 21 M. Jackson and H. H. Mantsch, *Crit. Rev. Biochem. Mol. Biol.*, 1995, **30**, 95–120.
- 22 W. K. Surewicz and H. H. Mantsch, *Biochim. Biophys. Acta, Protein Struct. Mol. Enzymol.*, 1988, **952**, 115–130.
- 23 M. Jackson and H. H. Mantsch, *Can. J. Chem.*, 1991, **69**, 1639–1642.
- 24 J. Rodrigues, D. Meier, O. Faix and H. Pereira, *J. Anal. Appl. Pyrolysis*, 1999, **48**, 121–128.

